

Dosimetric characterization of CyberKnife radiosurgical photon beams using polymer gels

E. Pantelis^{a)} and C. Antypas

Medical Physics Department, Iatropolis — Magnitiki Tomografia Clinic and Diagnostic Center, Ethnikis Antistaseos 54-56, Chalandri, 152 31, Athens, Greece

L. Petrokokkinos

Nuclear and Particle Physics Section, Physics Department, University of Athens, Panepistimioupolis, Ilisia, 157 71 Athens, Greece and Institute of Accelerating Systems & Applications (IASA), PO Box 17214, GR-10024 Athens, Greece

P. Karaikos and P. Papagiannis

Medical Physics Laboratory, Medical School, University of Athens, 75 Mikras Asias, 115 27 Athens, Greece

M. Kozicki

Faculty of Textile Engineering and Marketing, Department of Textile Finishing, Technical University of Lodz, Zeromskiego 116, 90-543 Lodz, Poland

E. Georgiou

Medical Physics Laboratory, Medical School, University of Athens, 75 Mikras Asias, 115 27 Athens, Greece

L. Sakelliou

Nuclear and Particle Physics Section, Physics Department, University of Athens, Panepistimioupolis, Ilisia, 157 71 Athens, Greece and Institute of Accelerating Systems & Applications (IASA), PO Box 17214, GR-10024 Athens, Greece

I. Seimenis

Medical Diagnostic Center Ayios Therissos, 92 Troodos Avenue, Strovolos, Nicosia, Cyprus

(Received 11 December 2007; revised 11 April 2008; accepted for publication 11 April 2008; published 14 May 2008)

Dose distributions registered in water equivalent, polymer gel dosimeters were used to measure the output factors and off-axis profiles of the radiosurgical photon beams employed for CyberKnife radiosurgery. Corresponding measurements were also performed using a shielded silicon diode commonly employed for CyberKnife commissioning, the PinPoint ion chamber, and Gafchromic EBT films, for reasons of comparison. Polymer gel results of this work for the output factors of the 5, 7.5, and 10 mm diameter beams are (0.702 ± 0.029) , (0.872 ± 0.039) , and (0.929 ± 0.041) , respectively. Comparison of polymer gel and diode measurements shows that the latter overestimate output factors of the two small beams (5% for the 5 mm beam and 3% for the 7.5 mm beams). This is attributed to the nonwater equivalence of the high atomic number silicon material of the diode detector. On the other hand, the PinPoint chamber is found to underestimate output factors up to 10% for the 5 mm beam due to volume averaging effects. Polymer gel and EBT film output factor results are found in close agreement for all beam sizes, emphasizing the importance of water equivalence and fine detector sensitive volume for small field dosimetry. Relative off-axis profile results are in good agreement for all dosimeters used in this work, with noticeable differences observed only in the PinPoint estimate of the 80%–20% penumbra width, which is relatively overestimated. © 2008 American Association of Physicists in Medicine.

[DOI: [10.1118/1.2919099](https://doi.org/10.1118/1.2919099)]

Key words: polymer gel dosimetry, film dosimetry, diode, output factor, CyberKnife

I. INTRODUCTION

Stereotactic radiosurgery (SRS) is a well-established treatment modality in the management of a wide variety of intracranial and, recently, extracranial lesions.^{1–5} In SRS, small field sizes and an increased number of beams aiming at the target from different directions are employed to create highly conformal dose distributions that are accurately registered with the target using stereotactic frames or image guidance.

This allows for high doses to be delivered to the target in a single or a small number of fractions, sparing at the same time surrounding critical structures.

The quantities required to be measured for commissioning and quality assurance purposes of a radiosurgery system include output factors (OF), off-axis ratios (OARs), and relative depth dose data. It is well recognized that the measurement of OFs and OARs are complicated due to the lateral electronic disequilibrium and the steep dose gradients in-

volved in a large portion of the fields used.^{6–10} Adequate detector resolution, minimum radiation field perturbation, tissue equivalence, integrating character, stable dose response that is also preferred to be linear and reproducible, as well as energy and dose rate independence should be the main features that the ideal dosimeter for small field dosimetry must possess.^{7,9,11–14} Currently, no single detector meets all the requirements for small field dosimetry;^{15–21} therefore, the use of several detector types for stereotactic beam data acquisition has been suggested as “good practice.”²² For field sizes less than 12.5 mm,⁹ in particular, significant deviations can be observed among the OF and off-axis profiles reported in the literature. These are not only attributed to the specific drawbacks of the different dosimetry systems used (dose rate dependence, nontissue equivalence, directional dependence, Cerenkov radiation, and poor reproducibility of diamond detectors, diode, MOSFETs, plastic scintillators, and films, respectively^{7–9,15,19,21}), but also to volume averaging effects.^{9,23,24} Different approaches have been proposed to address this problem including mathematical methods for the deconvolution of detector size,^{24–26} measurements of the same OF and/or dose off-axis profile using detectors of different size followed by extrapolation to zero volume,^{20,27} as well as Monte Carlo simulation.^{21,28} However, measurements with detectors of different size are time- and labor intensive, even if the availability of different detectors is warranted in the clinic, while there is always the need for the experimental verification of Monte Carlo data to account for subtle variations between different radiotherapy units of the same type.

Polymer gels may not be considered standard dosimeters yet due to problems associated mainly with individual point uncertainty, reproducibility, and the relatively advanced data processing skills they necessitate. Polymer gel dosimetry however has been successfully employed in small field dosimetry^{24,27,29–32} on the basis of its favorable characteristics such as the water equivalence of the gel substance³³ and the absence of radiation field perturbation, since the gel comprises both the phantom and the detector material.^{24,27,29–32} Moreover, studies based on a systematic modulation transfer function (MTF) approach have shown that a submillimeter resolution in polymer gel dose measurements can be achieved when MRI with a submillimeter acquisition resolution is used for the readout of the radiation-induced polymerization.^{34,35}

In this work the polymer gel–MRI dosimetry method was used to measure the OFs and dose off-axis profiles of the small circular stereotactic photon beams produced by a fourth generation (G4) CyberKnife image-guided robotic radiosurgery system (AccurayTM Inc., Sunnyvale, CA).^{3,21,36,37} Corresponding measurements were also performed using a shielded silicon diode, which is most commonly employed for CyberKnife commissioning purposes, a PinPoint ion chamber, and Gafchromic EBT films. Results of this work were compared to those of similar studies reported in the literature.

II. MATERIALS AND METHODS

II.A. Diode and ion chamber measurements

The output factor (or total scatter factor) used in CyberKnife dosimetry is defined as the ratio of dose per monitor unit (MU) for a radiosurgical beam of diameter s , to the corresponding dose per MU for the reference beam of 60 mm in diameter, at 15 mm depth inside the water medium, and for a given source to axis distance (SAD). OAR is defined as the ratio of dose per MU at off-axis distance r to the corresponding dose per MU at the center of the radiosurgical beam, for given SAD and water depth values.

A shielded, p -type silicon diode (PTW, TW60008, 1 mm² cross section and 2.5 μ m thickness) and a small, sensitive volume ion chamber (PTW, PinPoint[®] TW31014, 0.015 cm³ volume, 2 mm diameter, and 5 mm length) were used for dosimetry measurements performed in this work. The silicon diode and ion chamber employed for measurements in this work are widely used in small field dosimetry, and their respective advantages and disadvantages are well documented.^{7,9,18–21,23} Practical problems related to measurements using point detectors include accurate positioning that requires careful handling and setup of the detector. To suppress this type of uncertainty, each detector was situated at 15 mm depth inside an MP3 motorized water phantom with its stem parallel to the beam axis using a PTW-TRUFIX attachment system and aligned to the measuring point along the beam axis by exploiting the symmetry of the off-axis beam profiles acquired at 15 and 50 mm depths, respectively. For OF measurements, SAD was set to 800 mm and the CyberKnife 6MV circular stereotactic photon beams of 5, 7.5, 10, and 60 mm diameter were used to deliver the same number of monitor units (300 MU). The created charge for the 5, 7.5, and 10 mm beams was measured using a PTW-UNIDOS electrometer and divided with the corresponding reading for the 60 mm reference beam to calculate the OF for each beam size. For OAR measurements, each detector was placed at 15 mm depth and irradiated at 800 mm SAD. Two scans were performed for each beam size along two orthogonal directions perpendicular to the beam axis. The created charge was collected by a PTW-TANDEM dual-channel electrometer and corrected for beam output fluctuations using a reference chamber (PTW, Semiflex chamber TW31010, 0.125 cm³ sensitive volume) situated before the secondary collimator. The PTW-MEPHYSTO MCC software was used to average readings at the same off-axis distance, r , from the two acquired orthogonal off-axis profiles and normalize the averaged values to that obtained at the center of each beam. Following this procedure, half-averaged OAR profiles as a function of distance away from the central beam axis were finally obtained.

II.B. Gafchromic EBT film measurements

Gafchromic EBT films (ISP, Wayne, NJ)^{19,38} were used for film measurements performed in this work. The calibration curve of the specific film batch used (lot #: 35322–004I) was obtained beforehand by irradiating 16 precut EBT films

using the 60 mm reference beam with doses ranging from 10 to 750 cGy. For OF and OAR measurements, pre-cut EBT films of the same batch were positioned vertically to the central beam axis, at 15 mm depth within RW3 solid water slabs of 30×30×20 cm dimensions and irradiated from 800mm SAD using the 5, 7.5, 10, and 60 mm in diameter radiosurgical beams. A dose of 300 cGy was delivered to each film using the diode measured OF values in order to induce similar optical density on each film surface.

All EBT films were scanned 1 day postirradiation to allow postirradiation optical density growth, using an Epson Expression 1680Pro flatbed optical scanner. The Epson scanner was used in transmission mode and all films were scanned in 48-bit RGB mode with a resolution of 150 dpi (pixel size = 0.169 mm), but only the red color channel of the image was used and saved in tagged image file format (.tiff).¹⁹ The films scanned (all the irradiated and a nonirradiated film taken by the same batch) were placed in the same area of the scanner bed, maintaining the same orientation throughout the scanning procedure. Custom-written routines were employed to: (a) subtract the nonirradiated film optical density on a pixel by pixel basis to account for scanner nonuniformity; (b) calculate the coordinates of the center of each beam by exploiting the circular symmetry of the radiation field depicted on the film's plane; and (c) convert the net pixel values of each film to corresponding dose results using the calibration curve of the specific film batch.

In an effort to suppress individual point uncertainties, the dose at the radiation field center of the 5, 7.5, and 10 mm beams was calculated by averaging the dose values of 9 pixels lying within a square of 0.51 mm side, centered on the central pixel of each radiation field. Similarly, the dose at the center of the reference 60 mm beam was calculated by averaging the dose values of 100 pixels lying within a square of 1.7 mm side centered on the central pixel of the specific field. The dimensions of the areas within which dose was averaged for each beam were chosen based on the beam sizes so as to preclude averaging effects. Correspondingly, the dose value at each off-axis distance, r , was calculated by averaging the dose values of 11 pixels symmetrically distributed on a circle centered on the radiation beam center with a radius equal to the off-axis distance, r .

According to the irradiation technique followed in this work, the ratio of the dose values at the center of each radiosurgical beam to the corresponding dose of the 60 mm reference beam gives the deviation between the film and diode OF values, or equivalently, the correction factor that should be applied on the diode OF values to obtain the corresponding film results. Off-axis ratio values were calculated by dividing the mean dose values at each distance, r , to the corresponding dose at the center of each radiation beam. Propagation of uncertainty expressed by the standard deviation of mean dose values yielded an estimate for EBT measured OFs and OARs on the order of 0.5%.

II.C. Polymer gel measurements

The polymer gel dosimeter used in this study is a modification of the VIPAR gel formulation.^{29,30,39} VIPAR gels ex-

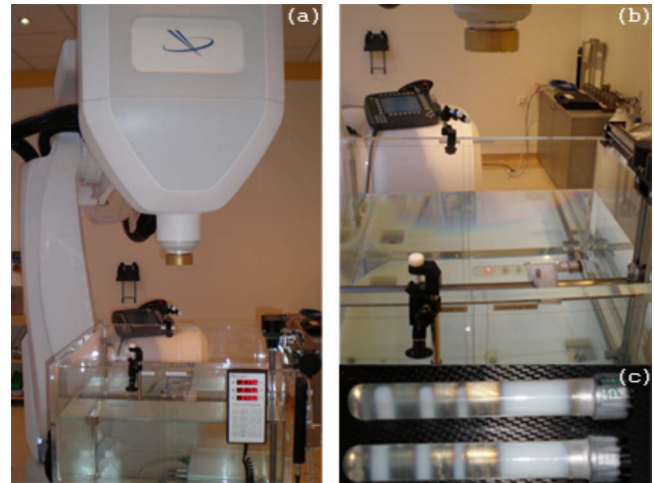


FIG. 1. (a), (b) Photographs showing the experimental setup for polymer gel dosimetry. (c) Photograph of the two irradiated gel vials immediately after their irradiation with the CyberKnife radiosurgical beams.

hibit an exceptionally wide dose response range with a linear part extending up to 45 Gy.³⁹ The modified gel was developed in an effort to maintain the favorable characteristics of the original VIPAR gel while decreasing the low dose threshold of the linear dose response range and, at the same time, facilitating its manufacturing procedure in normal atmospheric conditions without the need for cumbersome deoxygenation procedures, through the addition of appropriate oxygen scavengers.⁴⁰ This modified gel formulation (8% NVP, 4% MBA, 5% gelatin, 0.0008% CuSO₄, and 0.007% ascorbic acid) will be referred to as VIP in the following (i.e., the last two letters in the acronym for the original VIPAR that refer to the use of argon in the manufacturing procedure are dropped).

Following preparation, the gel solution was transferred to four Pyrex[®] cylindrical containers; two of 150 mm height, 23 mm inner diameter, and 2.5 mm wall thickness used for CyberKnife irradiations and two of 95 mm height, 45 mm inner diameter, and 2.5 mm wall thickness with a flexible, closed-end catheter of 1.5 mm external diameter (Nucletron BV, The Netherlands) introduced through an appropriate hole drilled into their cap, for irradiations using a Nucletron microSelec-tron ¹⁹²Ir HDR afterloader. All gel vials were hermetically sealed and stored overnight at room temperature to solidify.

For CyberKnife irradiations each vial was fixed in an MP3 motorized water phantom (PTW Freiburg, Germany) with its long axis lying parallel to the water surface and vertical to the central beam axis, as this was defined by the Linac laser [Figs. 1(a) and 1(b)]. The 60, 5, 7.5, and 10 mm radiosurgical beams were used to deliver the same dose of 30 Gy at 15 mm depth and at four different areas along each vial's long axis using the corresponding diode measured OFs. The centers of the 5, 7.5, and 10 mm beams were delivered at distances of 60, 85, and 115 mm, relative to the center of the 60 mm beam using the motorized mechanism of the water phantom. This irradiation scheme ensures minimum cross talk between adjacent irradiated areas of the do-

simeter (less than 1%, estimated using the beam off-axis profile data). A photograph of the two gel vials just after irradiation is shown in Fig. 1(c), and the radiation-induced polymerization of the gel substance is visible. Brachytherapy irradiations were performed on the same day using the microSelectron mHDR-v1 ^{192}Ir source to deliver 10 Gy at 1 cm distance along the transverse bisector of the source in its single dwell position.

MRI readout of the irradiated gel vials was performed 4 days postirradiation on a 3 T Philips Achieva MR scanner (Philips Medical Systems, Nederland BV). The same volume selective, Carr-Purcell-Meiboom-Gill (CPMG), 24-echo pulse sequence [with an initial echo time (TE) of 40 ms, with further 40 ms increments, and a repetition time (TR) of 3000 ms] was used for imaging the CyberKnife and brachytherapy gel vials in two separate sessions. A built-in quadrature radio-frequency (rf) body coil and a phased-array rf head coil were used for proton excitation and signal detection, respectively. The gel vials were placed at the center of the receiver coil in order to minimize rf field inhomogeneity effects. A rectangular field of view (FOV) covering an area of (169×169) mm², as well as an image acquisition and reconstruction matrix of 336×336 , were used, resulting in an in-plane acquisition resolution of 0.5×0.5 mm. A total number of 41 coronal partitions of 0.5 mm thickness were reconstructed for each echo depicting circular irradiation fields for both CyberKnife gel vials. Interpolation was not implemented, resulting in an isotropic acquisition voxel size of 0.5 mm³. This small voxel size ensures submillimeter spatial resolution dose measurements, since studies based on a systematic MTF approach have shown that the spatial resolution in polymer gel dosimetry is similar to the MRI acquisition resolution for pixel sizes down to 0.4 mm³.^{34,35} Sensitivity encoding was applied in the phase encoded direction to render the scanning feasible by reducing the total amount of data in the scan by a factor of 2. The receiver bandwidth was set to 220 Hz per pixel to reduce susceptibility effects, while two averages were used to boost SNR. An appropriate quality assurance procedure with a T_2 -weighted pulse sequence and the ACR phantom preceded the gel scanning, ensuring that image quality, as well as geometric and positioning accuracies, reflects high levels of system performance.

A single T_2 map (an image on which pixel signal intensity represents the NMR spin-spin relaxation time T_2 of the corresponding gel voxel) was calculated for each slice by fitting a simple log-linear function on the acquired 24-echo train on a pixel by pixel basis, after discarding the first echo due to imperfections in the signal decay curve.⁴¹ The resulting 41 T_2 maps were combined to construct a three-dimensional relaxation rate, $R_2(=1/T_2)$ matrix for each gel vial. The calculated 3D R_2 matrices allow for the reconstruction of the scanned volume in axial, coronal, sagittal, or in any chosen oblique plane.

Custom-made optimization routines based on the eccentricity and the center of mass of the radiation beams on different slices along the beam axis were employed to reconstruct the 3D R_2 matrices of each gel vial so that

radiosurgical beams were depicted as circles in each coronal plane, with their center of mass coinciding with the central beam axis. It should be noted that, since the 60 mm beam was not fully included in the irradiated gels [see Figs. 2(a) and 2(b)], only the 5, 7.5, and 10 mm beams were used for the reconstruction of the 3D R_2 matrix of each gel vial. The medial slice of the 41 reconstructed coronal slices was assumed to include the long axis of each vial, lying at 15 mm depth according to the irradiation setup. Uncertainty associated with the selection of the medial coronal slice lying at 15 mm depth is on the order of ± 1 slice (i.e., 0.5 mm) which, taking into account the relatively small dose gradient along the beam axis, does not affect the results of this work.

Given that the same dose was delivered for each beam size in both gel vials using the diode measured OFs, and assuming that this dose value lies in the linear dose response range of the VIP gel (i.e., $R_2 = a \cdot D + b$), the polymer gel result for the OF of each radiosurgical beam, s , can be calculated as the correction that should be applied to the corresponding diode OF according to

$$\text{OF}_s = \frac{R_{2,s}(r=0 \text{ mm}) - b}{R_{2,60 \text{ mm}}(r=0 \text{ mm}) - b} \times \frac{\text{TMR}_{60 \text{ mm}}(17.8 \text{ mm})}{\text{TMR}_s(17.8 \text{ mm})} \times \text{OF}_s^{\text{diode}}, \quad (1)$$

where $R_{2,s}(r=0 \text{ mm})$ and $R_{2,60 \text{ mm}}(r=0 \text{ mm})$ stand for the relaxation rate values at 15 mm depth and at the center of the stereotactic beam s and the reference 60 mm beam, respectively. $\text{TMR}_s(17.8 \text{ mm})$ and $\text{TMR}_{60 \text{ mm}}(17.8 \text{ mm})$ stand for the tissue to maximum ratio values for the radiosurgical beam s and the 60 mm reference beam, respectively, at water equivalent depth of 17.8 mm (taking into account the physical density and $\langle Z/A \rangle$ of Pyrex 2.23 g/cm^3 , 0.497, and the VIP gel 1.031 g/cm^3 , 0.551).³³

Experimental results following Eq. (1) do not depend on the sensitivity of VIP gel dose response, a , and depend only slightly on TMR ratios that vary between 0.987 and 1.002 for the 5 and 60 mm. The uncertainty associated with OF measurements can be derived using error propagation of the uncertainties in diode measured OF and TMR values (0.4%), the linear dose response intercept, b , and the R_2 values at the center of the irradiated beams.

Polymer gel dosimetry relying on single voxel estimates of the R_2 values at the center of the irradiated beams is expected to suffer by increased uncertainty. While the imaging voxel employed in this work (0.5 mm^3) is not affected by volume averaging effects, results of multiple voxels cannot be averaged to reduce uncertainty for the smaller beam sizes (i.e., 5, 7.5, and 10 mm). Reducing the imaging voxel would render the duration of the imaging session impractical; hence, a different approach had to be followed. The R_2 values at the center of the 5, 7.5, and 10 mm beams were calculated by averaging six interpolated R_2 values at the center of each beam. These values were obtained by choosing six off-axis profiles (i.e., an increment of 30° was used) and fitting a fifth-order polynomial to R_2 data on each profile lying at off-axis distances within the full width at half-

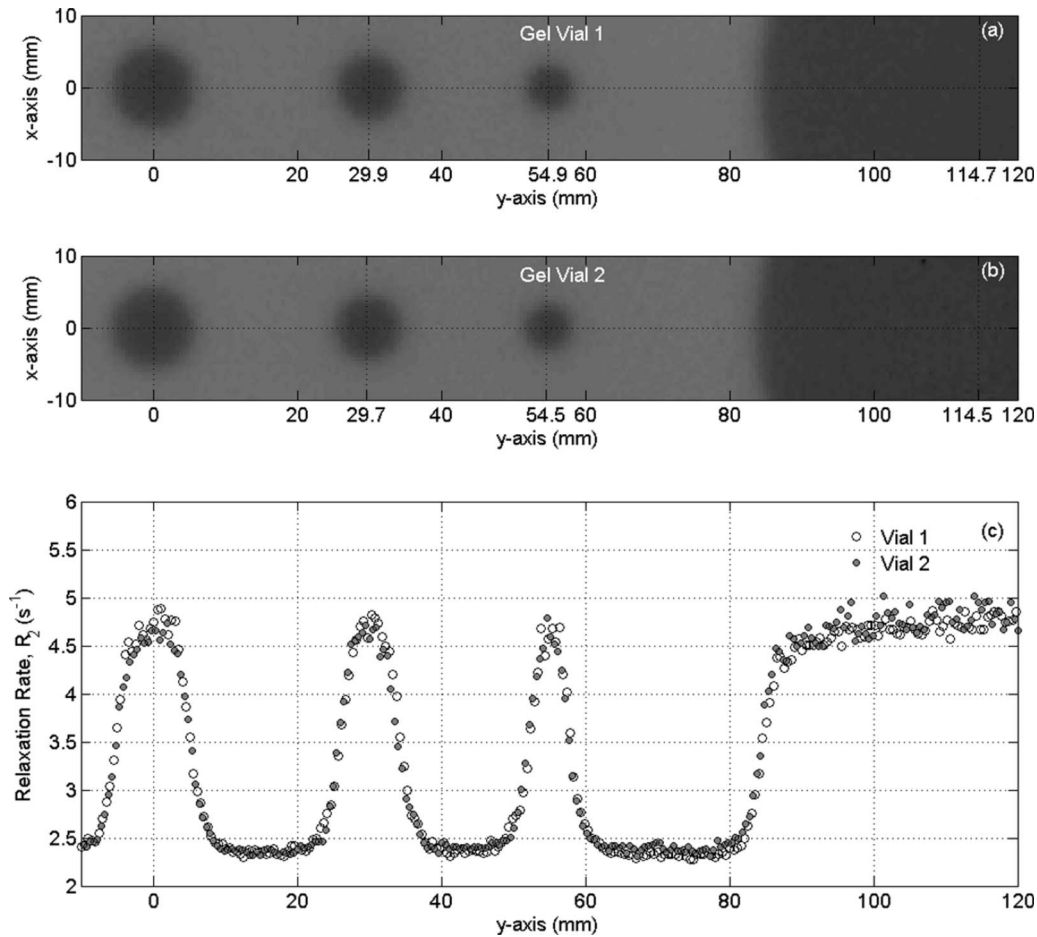


FIG. 2. (a), (b) The medial T_2 maps of the CyberKnife gel irradiated vials corresponding to a plane perpendicular to the beam axis, at 15 mm depth inside the water phantom. The experimentally defined beam center coordinates on these planes are also marked on the used coordinate system. (c) R_2 profiles measured in both gel vials along the y axis at $x=0$ mm.

maximum for each beam size. Following this approach, the uncertainty of the R_2 value at the center of each beam is less than 1.5%, which is lower than the 4% uncertainty of the corresponding R_2 value of the central voxel.

Regarding the 60 mm reference beam that was not fully registered in the irradiated gel vials, its center coordinates were found by the average of three values calculated by the experimentally defined centers of the 5, 7.5, and 10 mm beams and their distance relative to the center of the 60 mm beam as planned for the irradiation. Given the small plateau region of the off-axis profile for this specific beam size, the R_2 value at the center of the 60 mm beam was then calculated by averaging the R_2 values of 25 voxels lying within a square of 2.5 mm side centered on the central voxel. This approach yielded a statistical uncertainty of 2%.

For the purpose of OAR measurements, the R_2 value at a distance, r , away from the beam axis was calculated by averaging 11 R_2 values lying on a circle centered on the corresponding radiation beam center and with radius equal to the off-axis distance, r . OAR values as a function of distance, r , were then calculated according to

$$\text{OAR}(r) = \frac{R_{2,s}(r) - b}{R_{2,s}(r=0 \text{ mm}) - b}, \quad (2)$$

for each radiosurgical beam of diameter s . The uncertainty of each OAR value was calculated by propagating according to Eq. (2) the uncertainties of the mean R_2 values at off-axis distance, r , the $R_{2,s}(r=0 \text{ mm})$ at the center of each beam, and the intercept b of the linear dose response curve.

III. RESULTS AND DISCUSSION

In Figs. 2(a) and 2(b), the T_2 maps of each CyberKnife gel vial, lying perpendicular to the beam axis at 15 mm depth inside the water phantom, are presented using the same Cartesian coordinate frame. The origin of the employed frame coincides with the experimentally derived center for the 10 mm beam. In this system the z axis coincides with the beam axis, the y axis runs across the centers of the irradiated beams toward the vial's top, and the x axis is the vertical axis relative to the y and z axes. A general inspection of the presented T_2 maps implies that similar T_2 values are measured for all presented radiation fields in both gel vials without any

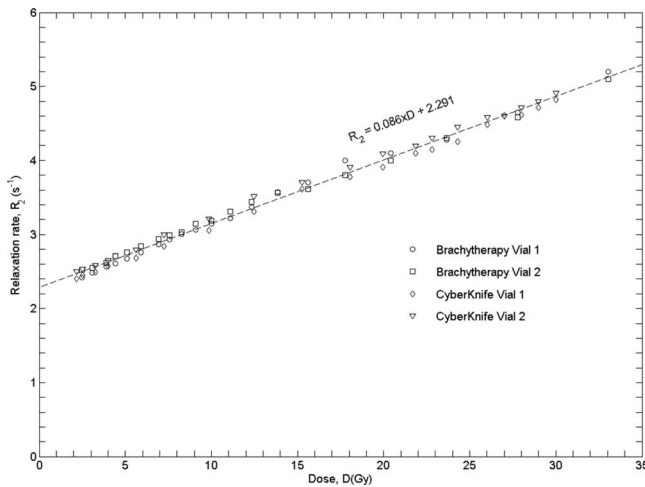


FIG. 3. Dose response data of the VIP gel formulation calculated using the gel vials irradiated with the ^{192}Ir HDR afterloader as well as using the 60 mm relative off-axis profiles of the two CyberKnife gel vials. The result of a linear fit to the four data sets presented is also presented.

cross talk between adjacent irradiated areas. The relative distances measured from the center of the 5 mm to the center of the 7.5 mm beam and from the center of the 7.5 mm to the center of the 10 mm beam were found equal to 25 and 29.9 mm in vial 1, and 24.8 and 29.7 mm in vial 2, respectively. These results are in excellent agreement (better than 1%) with the programmed values (see Sec. II C). Since the uncertainty of the motorized mechanism is less than 0.1 mm, this finding characterizes the experimental uncertainty in the beam center estimation. In Fig. 2(c) the measured R_2 profiles along the y axis of each gel vial are presented; a generally good agreement between the maximum R_2 values of each beam can be observed in both vials.

Dose response data of the VIP gel formulation were derived using the two calibration gel vials irradiated with the ^{192}Ir HDR afterloader, as well as the off-axis profiles of the 60 mm beam at 15 mm depth of the two gel vials irradiated

with the CyberKnife radiosurgical beams. Results are presented in Fig. 3, where a good agreement between the four data sets can be observed. Figure 3 shows that the VIP gel batch in this study presents a linear dose response region extending from 2Gy up to at least 35Gy, as the latter is confirmed by the brachytherapy calibration gel vials.

A linear fit on the dose response using all four data sets presented in Fig. 3 ($R_2 = a \cdot D + b$) yielded a sensitivity value, a , of $(0.086 \pm 0.002) \text{ s}^{-1} \text{ Gy}^{-1}$ and an intercept, b , of $(2.29 \pm 0.03) \text{ s}^{-1}$. A corresponding fitting procedure using the dose response data set of each CyberKnife gel vial yielded results in close agreement [sensitivity values of $(0.086 \pm 0.002) \text{ s}^{-1} \text{ Gy}^{-1}$ and $(0.085 \pm 0.002) \text{ s}^{-1} \text{ Gy}^{-1}$, and intercept values of $(2.22 \pm 0.03) \text{ s}^{-1}$ and $(2.34 \pm 0.04) \text{ s}^{-1}$ for vials 1 and 2, respectively]. In order to preclude potential systematic uncertainties related to small discrepancies between experimental and calibration gel vials, the calibration curves of each CyberKnife vial were used to derive polymer gel results of this work.

III.A. Output factors

R_2 values measured at the experimentally defined, central voxel for the 5 mm beam were found equal to $(4.725 \pm 0.189) \text{ s}^{-1}$ and $(4.681 \pm 0.187) \text{ s}^{-1}$ for vials 1 and 2, respectively. Using the calibration curve for each gel vial, these R_2 values can be translated to dose values of $(29.1 \pm 1.4) \text{ Gy}$ and $(27.5 \pm 1.3) \text{ Gy}$, which agree within errors and yield an average of $(28.3 \pm 1.4) \text{ Gy}$. Following the same procedure, average dose values were found equal to $(29.2 \pm 1.5) \text{ Gy}$ and $(30.1 \pm 1.5) \text{ Gy}$ for the 7.5 and 10 mm beams. Given that the irradiation was planned to deliver 30 Gy for all beams using the diode measured OFs, these values imply an OF overestimation for the 5 and 7.5 mm beams. Definitive conclusions cannot be drawn however due to the significant uncertainties involved in this approach.

Estimating the average R_2 value at the center of each beam following the procedure described in Sec. II C to re-

TABLE I. Output factor measurements for the 5, 7.5, and 10 mm diameter, circular, radiosurgical beams of the CyberKnife system. Corresponding data reported in the literature are also shown for comparison.

Detector type		Output factor		
		5.0 mm	7.5 mm	10 mm
Polymer gel	(This work)	0.702 ± 0.029	0.872 ± 0.039	0.929 ± 0.041
	PTW 60008 diode			
	(This work)	0.737 ± 0.003	0.899 ± 0.004	0.932 ± 0.004
	(Ref. 18)	0.719 ± 0.015	0.849 ± 0.011	0.892 ± 0.011
	(Ref. 19)	0.706 ± 0.002	0.869 ± 0.002	0.911 ± 0.002
	(Ref. 21)	0.746	0.878	0.916
PTW PinPoint	(This work)	0.634 ± 0.003	0.802 ± 0.004	0.857 ± 0.004
	(Ref. 21)	0.642	0.804	0.860
Gafchromic EBT	(This work)	0.707 ± 0.005	0.850 ± 0.005	0.903 ± 0.005
	(Ref. 19)	0.701 ± 0.002	0.845 ± 0.002	0.902 ± 0.002
PTW diamond	(Ref. 21)	0.640	0.878	0.916
	TLD	(Ref. 18)	0.672 ± 0.025	0.816 ± 0.026
GRD	(Ref. 17)	0.711 ± 0.021	0.851 ± 0.027	...
Monte Carlo	(Ref. 21)	0.701	0.838	0.877

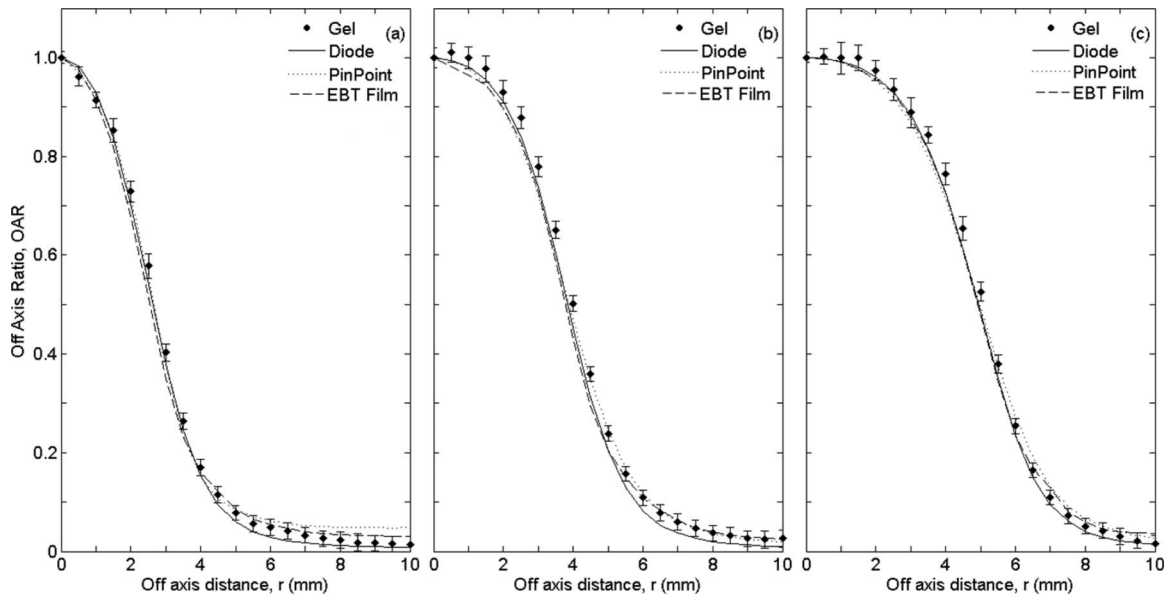


FIG. 4. Polymer gel, diode, PinPoint, and EBT measured OAR values plotted vs off-axis distance, r (mm) for the circular, CyberKnife radiosurgical beams of (a) 5 mm; (b) 7.5 mm; and (c) 10 mm diameter.

duce uncertainties, and using Eq. (1) yields the OF results summarized in Table I corresponding to the average OF for each beam, from both gel vials. Table I also presents measurements of this work employing the shielded silicon diode that is widely used for CyberKnife commissioning, the Pin-Point chamber, and Gafchromic EBT films, as well as corresponding OF results in the literature measured using a variety of detectors and calculated by Monte Carlo computational methods, for reasons of comparison.

Polymer gel data presented in Table I show that, while diode measurements agree within errors for the 10 mm beam, they overestimate OFs by 5% for the 5 mm beam and 3% for the 7.5 mm beam, which is consistent with single voxel results presented above. Given that the polymer gel and EBT film results shown in Table I are in close agreement, the diode OF overestimation is most probably due to the nonwater equivalence of the diode detector. This is also supported by findings of Haryanto *et al.*,⁴² where a close agreement is found between calculated and measured output factors when the water material of the detector voxel in their Monte Carlo simulations is replaced by silicon. Araki²⁸ used Monte Carlo simulations to show that the silicon detector causes a reduction in lateral electronic disequilibrium due to its higher density and atomic number relative to water, which results in an overestimation of the output factor for the 5 and 7.5 mm beams on the order of 5%.

Regarding PinPoint OF results of this work, an underestimation which stretches up to 10% for the 5 mm beam can be seen in Table I relative to corresponding polymer gel values. This is mainly attributed to the volume averaging effect, which is of increased importance in dosimetry measurements of small, pointed-shape photon beams.²⁰

Polymer gel and EBT OF results of this work summarized in Table I are in good agreement for all beam sizes. This emphasizes the importance of water equivalence and fine de-

tector sensitive volume of detectors used for small field dosimetry where steep dose gradients and lack of lateral electronic equilibrium exist.

Findings of this work regarding the accuracy of OF measurements using different dosimeters for the 5 and 7.5 mm beams are in agreement with previous studies comparing Monte Carlo simulations²¹ and water equivalent diamond²¹ or TLD measurements,¹⁸ to corresponding diode measured OFs. The only contradicting study is Ref. 19, where an OF overestimation of diode measurements is shown relative to EBT film results for the 7.5 mm beam, but not for the 5 mm beam.

Besides the general trend of relative diode OF overestimation and relative PinPoint OF underestimation, comparison between absolute diode OF values measured in this work and corresponding results reported in the literature shows significant variations for all beam sizes. However, such a comparison is of relatively limited value since, besides potential experimental uncertainties that are mainly associated with the exact positioning of the detector, the observed differences can also be attributed to systematic uncertainties originating from the manufacturing variation in the secondary collimator dimensions, as well as small differences in the electron beam width in different CyberKnife systems. Regarding the latter, Francescon *et al.* recently reported that a difference of 0.5 mm in the electron beam width can cause a 4% variation in the output factor of the 5 mm beam.⁴³

III.B. Relative off-axis ratios

In Fig. 4 average polymer gel OAR values from both CyberKnife gel vials are presented as a function of off-axis distance, r , along with corresponding diode, PinPoint, and EBT measured values for the 5, 7.5, and 10 mm diameter radiosurgical beams. In general an agreement within experi-

TABLE II. Experimental results of this work using various dosimeters, for the 80%–20% penumbra and field size of the 5, 7.5, and 10 mm diameter, circular, radiosurgical beams of the CyberKnife system. Uncertainty of presented results is on the order of 0.02.

Detector type	80%–20% penumbra			Field size		
	5.0 mm	7.5 mm	10 mm	5.0 mm	7.5 mm	10 mm
Polymer gel	2.16	2.40	2.72	5.18	7.70	9.84
Diode	2.11	2.33	2.61	5.25	7.69	9.87
PinPoint	2.25	2.58	2.95	5.30	7.79	9.96
Gafchromic EBT	2.15	2.39	2.69	5.08	7.74	9.83

mental uncertainties can be observed between the polymer gel and the corresponding diode, PinPoint, and EBT data sets.

A more quantitative approach involves the calculation of the 80%–20% penumbra and the field size of the measured radiosurgical beams. Cubic spline interpolations on the OAR data sets presented in Fig. 4 were used for the calculation of the penumbra and field size values, with the latter being calculated as double the off-axis distance that corresponds to the 0.5 OAR value. Results are summarized in Table II for the measured beams and the polymer gel, diode, PinPoint, and EBT dosimetry systems. A general good agreement between the polymer gel measured penumbra values with the corresponding diode and EBT results can be observed. PinPoint measured penumbra values on the other hand were found increased by up to 8% for the 7.5 mm beam relative to corresponding polymer gel values, due to the importance of the volume averaging effect in these fields sizes. Regarding field size measurements, an agreement (within 4%) is observed between the polymer gel and the diode, PinPoint, and EBT data sets. Comparison of the measured field size values with the nominal 5, 7.5, and 10 mm values reveals that all the used dosimeters overestimate the size of the 5 and 7.5 mm beams, while they slightly underestimate the size of the 10 mm beam. Specifically, polymer gel results for the 5 and 7.5 mm beams were found 4% and 3% higher than corresponding nominal beam sizes, while the polymer gel measured field size of the 10 mm beam was underestimated by 3%. The observed differences could be attributed to the small geometrical uncertainties of the secondary collimator dimensions.

IV. CONCLUSIONS

The polymer gel–MRI method was used to measure the output factors and relative off-axis profiles of the 5, 7.5, and 10 mm diameter radiosurgical beams of a CyberKnife image-guided robotic SRS system. Results were compared to corresponding measurements of this work using a shielded silicon diode commonly employed for CyberKnife commissioning purposes, a PinPoint ion chamber, and Gafchromic EBT films. While gel and EBT film results were found in close agreement, an overestimation of 5% and 3% between polymer gel and diode measured OF values was observed for the 5 and 7.5 mm beams, respectively. This finding is mainly attributed to the water nonequivalence of

the high atomic number silicon material of the diode detector. The PinPoint chamber was found to underestimate output factors by up to 10% for the 5 mm beam due to volume averaging effects.

A direct comparison of OF results in the literature is of limited value due to potential manufacturing variations in the secondary collimator dimensions of different CyberKnife systems and associated differences in the emitted photon spectrum. Nevertheless, the trend of diode overestimation and PinPoint underestimation reported herein can also be seen in corresponding studies in the literature comparing Monte Carlo simulation results and measurements using water equivalent systems (i.e., films, TLD, and glass rod detectors) with diode and PinPoint results. This suggests that independent validation of diode measured OF values should be verified for each CyberKnife system using a dosimetry method which combines water equivalence and fine detector sensitive volume. Relative off-axis profile results of this work were found in good agreement for all different dosimeters employed with the exception of the PinPoint chamber, which results in a noticeable field size and penumbra broadening.

ACKNOWLEDGMENTS

This work was supported in part by a Greece–Poland joint research and technology program 2005–2007 by the Greek General Secretariat for Research & Technology (Program No. 184-E). Financial support from the Polish Ministry of Science and Higher Education (Grant No. N205 048 32/2930) is also appreciated.

^{a)} Author to whom correspondence should be addressed. Electronic mail: vpantelis@phys.uoa.gr

¹R. Wurm and P. Okunieff, “Intracranial and extracranial stereotactic radiosurgery and radiotherapy,” *Int. J. Radiat. Oncol. Biol. Phys.* **66**, S1–S2 (2006).

²B. D. Kavanagh and R. D. Timmerman, “Stereotactic radiosurgery and stereotactic body radiation therapy: An overview of technical considerations and clinical applications,” *Hematol. Oncol. Clin. North Am.* **20**, 87–95 (2006).

³P. Romanelli, D. W. Schaal, and J. R. Adler, “Image-guided radiosurgical ablation of intra- and extra-cranial lesions,” *Technol. Cancer Res. Treat.* **5**, 421–428 (2006).

⁴G. Strassmann, I. Braun, O. Kress, D. Richter, H. O. Neidel, K. J. Klose, H. An, B. Vogel, F. Rose, and R. Engenhart-Cabillic, “Accuracy of single-session extracranial radiotherapy for simple shaped lung tumor or metastasis using fast 3-D CT treatment planning,” *Int. J. Radiat. Oncol. Biol. Phys.* **66**, 576–582 (2006).

⁵Q. Wu, J. Liang, and D. Yan, “Application of dose compensation in

- image-guided radiotherapy of prostate cancer," *Phys. Med. Biol.* **51**, 1405–1419 (2006).
- ⁶A. Wu, R. D. Zwicker, A. M. Kallend, and Z. Zheng, "Comments on dose measurements for a narrow beam radiosurgery," *Med. Phys.* **20**, 777–779 (1993).
- ⁷M. Heydarian, P. W. Hoban, and A. H. Beddoe, "A comparison of dosimetry techniques in stereotactic radiosurgery," *Phys. Med. Biol.* **41**, 93–110 (1996).
- ⁸D. M. Duggan and C. W. Coffey II, "Small photon field dosimetry for stereotactic radiosurgery," *Med. Dosim.* **23**, 153–159 (1998).
- ⁹C. McKerracher and D. I. Thwaites, "Assessment of new small-field detectors against standard-field detectors for practical stereotactic beam data acquisition," *Phys. Med. Biol.* **44**, 2143–2160 (1999).
- ¹⁰K. A. Paskalev, J. P. Seuntjens, H. J. Patrocinio, and E. B. Podgorsak, "Physical aspects of dynamic stereotactic radiosurgery with very small photon beams (1.5 and 3 mm in diameter)," *Med. Phys.* **30**, 111–118 (2003).
- ¹¹R. K. Rice, J. L. Hansen, G. K. Svensson, and R. L. Siddon, "Measurements of dose distributions in small beams of 6 MV x-rays," *Phys. Med. Biol.* **32**, 1087–1099 (1987).
- ¹²C. F. Serago, P. V. Houdek, G. H. Hartmann, D. S. Saini, M. E. Serago, and A. Kaydee, "Tissue maximum ratios (and other parameters) of small circular 4, 6, 10, 15 and 24 MV x-ray beams for radiosurgery," *Phys. Med. Biol.* **37**, 1943–1956 (1992).
- ¹³C. Martens, C. De Wagter, and W. De Neve, "The value of the PinPoint ion chamber for characterization of small field segments used in intensity modulated radiotherapy," *Phys. Med. Biol.* **45**, 2519–2530 (2000).
- ¹⁴M. Westermark, J. Arndt, B. Nilsson, and A. Brahme, "Comparative dosimetry in narrow high-energy photon beams," *Phys. Med. Biol.* **45**, 685–702 (2000).
- ¹⁵P. Francescon, S. Cora, C. Cavedon, P. Scalchi, S. Reccanello, and F. Colombo, "Use of new type radiochromic film, a new parallel-plate micro-chamber, MOSFETS, and TLD 800 microcubes in the dosimetry of small beams," *Med. Phys.* **25**, 503–511 (1998).
- ¹⁶X. R. Zhu, J. J. Allen, J. Shi, and W. E. Simon, "Total scatter factors and tissue maximum ratios for small radiosurgery fields: Comparison of diode detectors, a parallel-plate ion chamber, and radiographic film," *Med. Phys.* **27**, 472–477 (2000).
- ¹⁷J. Perks, M. Gao, V. Smith, S. Skubic, and S. Goetsch, "Glass rod detectors for small field, stereotactic radiosurgery dosimetric audit," *Med. Phys.* **32**, 726–732 (2005).
- ¹⁸C. Yu, G. Jozsef, M. L. J. Apuzzo, and Z. Petrovich, "Measurements of the relative output factors for CyberKnife collimators," *Neurosurgery* **54**, 157–162 (2004).
- ¹⁹E. E. Wilcox and G. M. Daskalov, "Evaluation of GAFCHROMIC[®] EBT film for CyberKnife[®] dosimetry," *Med. Phys.* **34**, 1967–1974 (2007).
- ²⁰O. A. Sauer and J. Wilbert, "Measurement of output factors for small photon beams," *Med. Phys.* **34**, 1983–1988 (2007).
- ²¹P. Francescon S. Cora, C. Cavedon, P. Scalchi, and J. Stancanello, "CyberKnife Dosimetric Beam Characteristics: Comparison Between Experimental Results and Monte Carlo Simulation," in *Robotic Radiosurgery* (CyberKnife Society Press, Sunnyvale, CA, 2005), Vol. 1, pp. 271–280.
- ²²E. B. Podgorsak, "Physics for radiosurgery with linear accelerators," *Neurosurg. Clin. N. Am.* **3**, 9–34 (1992).
- ²³W. U. Laub and T. Wong, "The volume effect of detectors in the dosimetry of small fields used in IMRT," *Med. Phys.* **30**, 341–347 (2003).
- ²⁴E. Pappas, T. G. Maris, A. Papadakis, F. Zacharopoulou, J. Damilakis, N. Papanikolaou and N. Gourtsoyiannis, "Experimental determination of the effect of detector size on profile measurements in narrow photon beams," *Med. Phys.* **33**, 3700–3710 (2006).
- ²⁵P. D. Higgins, C. H. Sibata, L. Siskind, and J. W. Sohn, "Deconvolution of detector size effect for small field measurement," *Med. Phys.* **22**, 1663–1666 (1995).
- ²⁶C. H. Sibata, H. C. Mota, A. S. Beddar, P. D. Higgins, and K. H. Shin, "Influence of detector size in photon beam profile measurements," *Phys. Med. Biol.* **36**, 621–631 (1991).
- ²⁷E. Pappas, L. Petrokokkinos, A. Angelopoulos, T. G. Maris, M. Kozicki, I. Dalezios, and V. Kouloulis, "Relative output factor measurements of a 5mm diameter radiosurgical photon beam using polymer gel dosimetry," *Med. Phys.* **32**, 1513–1520 (2005).
- ²⁸F. Araki, "Monte Carlo study of a CyberKnife stereotactic radiosurgery system," *Med. Phys.* **33**, 2955–2963 (2006).
- ²⁹E. Pappas, I. Seimenis, A. Angelopoulos, P. Georgolopoulou, M. Kamariotaki-Papariopoulou, T. Maris, L. Sakelliou, P. Sandilos, and L. Vlachos, "Narrow stereotactic beam profile measurements using N-vinylpyrrolidone based polymer gels and magnetic resonance imaging," *Phys. Med. Biol.* **46**, 783–797 (2001).
- ³⁰P. Karaiskos, L. Petrokokkinos, E. Tatsis, A. Angelopoulos, P. Baras, M. Kozicki, P. Papagiannis, J. M. Rosiak, L. Sakelliou, P. Sandilos, and L. Vlachos, "Dose verification of single shot gamma knife applications using VIPAR polymer gel and MRI," *Phys. Med. Biol.* **50**, 1235–1250 (2005).
- ³¹P. Papagiannis, P. Karaiskos, M. Kozicki, J. M. Rosiak, L. Sakelliou, P. Sandilos, I. Seimenis, and M. Torrens, "Three-dimensional dose verification of the clinical application of gamma knife stereotactic radiosurgery using polymer gel and MRI," *Phys. Med. Biol.* **50**, 1979–1990 (2005).
- ³²J. Novotny, Jr., P. Dvorak, V. Spevacek, J. Tintera, J. Novotny, T. Cechak, and R. Liscak, "Quality control of the stereotactic radiosurgery procedure with the polymer-gel dosimetry," *Radiother. Oncol.* **63**, 223–230 (2002).
- ³³E. Pantelis, A. K. Karlis, M. Kozicki, P. Papagiannis, L. Sakelliou, and J. M. Rosiak, "Polymer gel water equivalence and relative energy response with emphasis on low photon energy dosimetry in brachytherapy," *Phys. Med. Biol.* **49**, 3495–3514 (2004).
- ³⁴A. Berg, A. Ertl, and E. Moser, "High resolution polymer gel dosimetry by parameter selective MR-microimaging on a whole body scanner at 3T," *Med. Phys.* **28**, 833–843 (2001).
- ³⁵A. Berg, M. Pernkopf, C. Waldhäusl, W. Schmidt, and E. Moser, "High resolution MR based polymer dosimetry versus film densitometry: A systematic study based on the modulation transfer function approach," *Phys. Med. Biol.* **49**, 4087–4108 (2004).
- ³⁶J. R. Adler, M. J. Murphy, S. D. Chang, and S. L. Hancock, "Image-guided robotic radiosurgery," *Neurosurgery* **44**, 1299–1307 (1999).
- ³⁷P. Romanelli, A. Schweikard, A. Schlaefler, and J. Adler, "Computed aided robotic radiosurgery," *Comput. Aided Surg.* **11**, 161–174 (2006).
- ³⁸M. Todorovic, M. Fischer, F. Cremers, E. Thom, and R. Schmidt, "Evaluation of GafChromic EBT prototype B for external beam dose verification," *Med. Phys.* **33**, 1321–1328 (2006).
- ³⁹P. Kipouros, E. Pappas, P. Baras, D. Hatzipanayoti, P. Karaiskos, L. Sakelliou, P. Sandilos, and I. Seimenis, "Wide dynamic dose range of VIPAR polymer gel dosimetry," *Phys. Med. Biol.* **46**, 2143–2159 (2001).
- ⁴⁰M. Kozicki, P. Maras, K. Rybka, T. Biegański, S. Kadłubowski, and L. Petrokokkinos, "On the development of the VIPAR polymer gel dosimeter for three-dimensional dose measurements," *Macromol. Symp.* **254**, 345–352 (2007).
- ⁴¹Y. De Deene, R. Van de Walle, E. Achten, and C. De Wagter, "Mathematical analysis and experimental investigation of noise in quantitative magnetic resonance imaging applied in polymer gel dosimetry," *Signal Process.* **70**, 85–101 (1998).
- ⁴²F. Haryanto, M. Fippel, W. Laub, O. Dohm and F. Nusslin, "Investigation of photon beam output factors for conformal radiation therapy—Monte Carlo simulations and measurements," *Phys. Med. Biol.* **47**, N133–N143 (2002).
- ⁴³P. Francescon, S. Cora, and C. Cavedon, "Total scatter factors of small beams: A multidetector and Monte Carlo study," *Med. Phys.* **35**, 504–513 (2008).